Pramāṇa–J. Phys., Vol. 31, No. 3, September 1988, pp. 173–184. © Printed in India.

Semi-classical approach to antiproton-nucleus scattering

B DEY, C S SHASTRY and T K ROY*

Department of Physics, North-Eastern Hill University, Shillong 793 003, India
*Theoretical Nuclear Physics Division, Saha Institute of Nuclear Physics, Calcutta 700 009, India

MS received 26 October 1987; revised 11 April 1988

Abstract. The similarities and differences between antiproton-nucleus scattering and heavy-ion-nucleus scattering are examined. It is found that the one-turning point approach viz Wentzel, Kramers and Brillouin (WKB) approximation can be applied to the analysis of antiproton-nucleus scattering. Using this approximation, a closed form expression for the nuclear phase shift is deduced from the corresponding expression for the heavy-ion scattering phase shift derived by Shastry and the method is illustrated by carrying out the cross-section calculation of $\bar{p} + {}^{40}Ca$ at $E_{lab} = 46{\cdot}8$ MeV.

Keywords. WKB approximation; antiproton scattering; heavy ion scattering; p-nucleus; nucleus-nucleus scattering.

PACS No. 25·40

1. Introduction

Major advances in our understanding of atomic nuclei have taken place as a result of detailed exploration of nuclei using a variety of probes like electrons, nucleons, deutrons and heavy-ions. During the last two decades, information generated by heavy-ion scattering (HIS) has evolved as a major area of nuclear physics. More recently, scattering and reaction experiments conducted on different nuclei using the antiproton ($\bar{p}$) as projectile have initiated a new line of exploration of the nuclei (Garreta *et al* 1984; Kronenfeld *et al* 1984; Mackellar *et al* 1984; Kubo *et al* 1985; Ingemarsson 1986; Janouin *et al* 1986) which is of much interest due to several reasons. These can provide a better idea of the interaction of antiprotons with nuclear matter, antiproton-nucleus potentials, additional reaction channels due to annihilation of antiproton etc. The experiments and theoretical calculations carried out so far provide interesting similarities between antiproton-nucleus scattering and heavy-ion nucleus scattering. Both of these are predominantly surface-dominated phenomena and in general, the inner regions of the interaction potentials are not uniquely determined. In both cases nuclei appear as highly absorptive spheres and the differential scattering cross-sections show characteristic diffraction patterns. The physical origin of the surface dominance in these cases, however, appears to be different. The heavy-ion scattering, in general, is dominated by a high Coulomb barrier. As a result, the interacting nuclei get slowed down in the barrier region and hence most of the reaction processes at low energy take place around the barrier region which makes the surface region of the potential comparatively well determined. Most of the partial waves below the grazing

partial wave get completely absorbed and hence, are not helpful in uniquely determining the potential in the interior region. On the other hand, the surface dominance of antiproton-nucleus scattering has a different origin. In this case there is no Coulomb barrier and for some partial waves there may be a very low barrier due to the centrifugal term. The surface dominance of the antiproton-nucleus scattering is due to a large number of additional channels that open up due to the annihilation process generated by the proton-antiproton collisions. The scattering wave gets strongly attenuated in the surface region due to these additional channels and hence, only limited information regarding the surface region of the interaction is possible.

These similarities indicate that techniques developed for the HIS (Frahn and Rehm 1978; Shastry 1982) may be usefully adopted in the analysis of the $\bar{p}$-nucleus scattering. In particular, in this problem we examine the usefulness of the WKB techniques and the closed-formalism approach for the study of $\bar{p}$-nucleus scattering. In §2 we make a comparative study of reflection functions and potentials in the heavy-ion scattering and antiproton-nucleus scattering. In §3 we develop the WKB technique to analyse the antiproton-nucleus scattering. Section 4 discusses typical numerical results obtained by this approach and describes the main conclusion.

2. Comparison of $\bar{p}$-nucleus and nucleus-nucleus scattering

We consider a typical case of heavy-ion scattering and compare it with the antiproton-nucleus scattering. The typical cases of heavy-ion and antiproton scattering considered are $^{18}O + {}^{58}Ni$ at $E_{lab} = 60$ MeV (Videbaek *et al* 1976) and $\bar{p} + {}^{40}Ca$ at $E_{lab} = 46{\cdot}8$ MeV (Heiselberg *et al* 1985). Both are analysed using phenomenological optical potentials. The expression used for the optical potential in both cases has the form

$$V(r) = -V_0 f(r, a_r, R_r) - iW_0 f(r, a_i, R_i) + U_c(r) = U_n(r) + U_c(r), \tag{1}$$

Table 1. Potential parameters for $^{18}O + {}^{58}Ni$, $\bar{p} + {}^{40}Ca$ and $\bar{p} + {}^{12}C$ systems. E is the centre-of-mass energy.

Systems	$^{18}O + {}^{58}Ni$ (a)	$\bar{p} + {}^{40}Ca$ (b)	$\bar{p} + {}^{12}C$ (c)
E_{lab}(MeV)	60·00	46·8	46·8
E (MeV)	45·79	45·66	43·2
k (fm^{-1})	5·49	1·46	1·38
η	19·32	−0·46	−0·138
V_0(MeV)	90·1	40·0	40·0
W_0(MeV)	42·9	100·0	74·1
r_r(fm)	1·22	1·1	1·03
r_i(fm)	1·22	1·1	1·07
a_r(fm)	0·5	0·6	0·562
a_i(fm)	0·5	0·6	0·625
r_c'(fm)	1·25	1·3	1·3

(a) Videbaek *et al* (1976); (b) Heiselberg *et al* (1985); (c) Kubo *et al* (1985)

where

$$f(r, a, R) = \left[1 + \exp\left(\frac{r - R}{a}\right)\right]^{-1}$$

$$U_c(r) = \frac{Z_P Z_T e^2}{2R_c}(3 - r^2/R_c^2) \quad r \leqslant R_c,$$

$$= (Z_P Z_T e^2)/r \qquad r \geqslant R_c. \tag{2}$$

In the case of heavy-ion scattering, the parameters R and R_c are given by

$$R = r(A_T^{1/3} + A_P^{1/3})$$

and

$$R_c = r_c'(A_T^{1/3} + A_P^{1/3}).$$

In the $\bar{p}$-nucleus scattering case $R = rA_T^{1/3}$ and $R_c = r_c' A_T^{1/3}$. The quantities r, r_c' are radius parameters. Z_P, Z_T are the atomic numbers of projectile and target, respectively and A_P and A_T are their respective mass numbers.

The effective potential corresponding to lth partial wave in radial Schrödinger

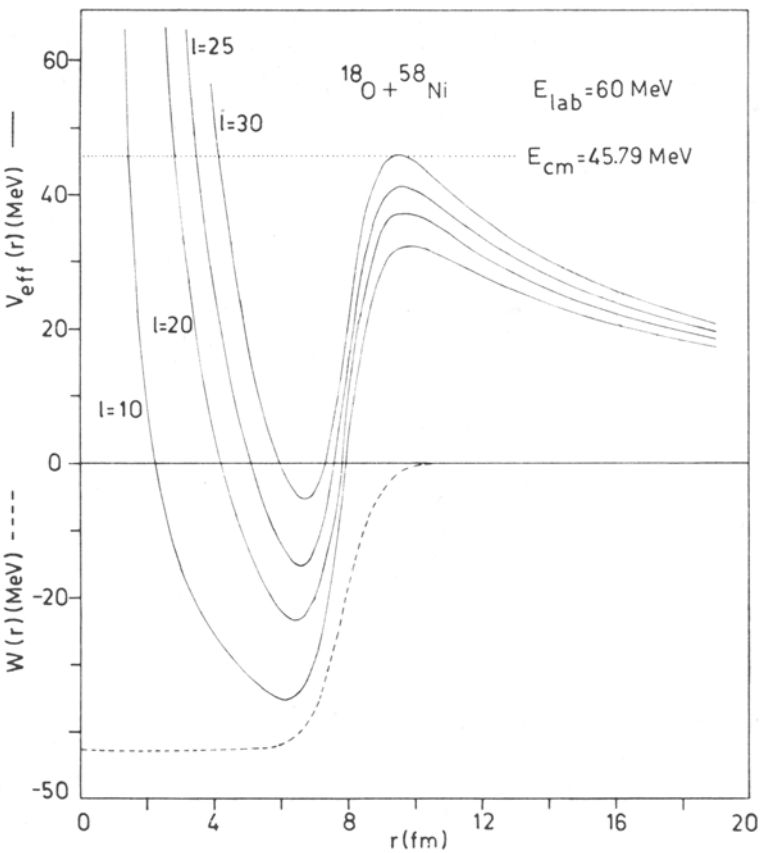

Figure 1a. Effective potentials as a function of r for the potential described in $^{18}O + ^{58}Ni$ scattering at $E_{lab} = 60$ MeV. Potential parameters are given in table 1.

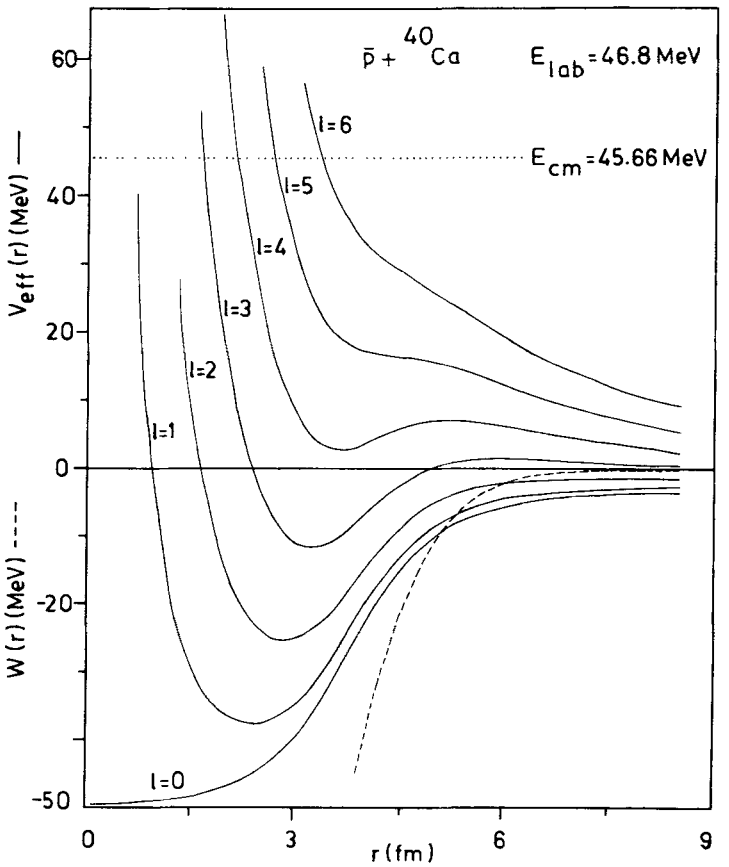

Figure 1b. Same as figure 1a for $\bar{p} + {}^{40}Ca$ scattering at $E_{lab} = 46{\cdot}8$ MeV. Potential parameters are given in table 1.

equation is

$$V_{eff}(r) = V(r) + \frac{\hbar^2}{2\mu}\frac{l(l+1)}{r^2} \tag{3}$$

where μ is the reduced mass. The optical model parameters and other relevant data are summarised in table 1.

From the comparison of effective potentials (figures 1a and 1b) of $^{18}O + {}^{58}Ni$ and $\bar{p} + {}^{40}Ca$ for different partial waves it is clear that both processes are governed by strongly absorptive imaginary part of the potential but the surface regions are not similar. In the heavy-ion system for a number of partial waves it is easy to identify the interior region, the barrier region and the outer region. In the antiproton-nucleus system the barrier near the surface is practically absent for almost all partial waves and even if present, are quite broad and shallow. The nature of the effective potential in heavy-ion scattering suggests, in general, a three-turning point WKB approach. On the other hand, in the antiproton-nucleus scattering there will be, in general, only one turning point corresponding to the interior part of the centrifugal term in the potential.

Table 2. Verification of WKB approximation for various values of l.

Systems	l	r (fm)	$\lambda(r)$ (fm)	$\lambda(r)\left\|\frac{dp}{dr}\right\|$ ($\times 10^{23}$) (MeV-s/fm)	$\|p(r)\|$ ($\times 10^{21}$) (MeV-s/fm)	$\left(\lambda(r)\left\|\frac{dp}{dr}\right\| \Big/ \|p(r)\|\right)$ ($\times 10^2$)
$^{18}O + {}^{58}Ni$	25	9·4	3·51	29·45	1·18	24·96
($E_{lab} = 60$ MeV)	20	9·7	2·68	23·74	1·54	15·35
$\bar{p} + {}^{40}Ca$	4	5·2	4·69	2·58	0·88	2·93
($E_{lab} = 46{\cdot}8$ MeV)	3	5·8	4·38	3·21	0·94	3·4

However, the comparatively smooth potential in the surface region suggests that the one-turning point WKB approach will be quite appropriate for the analyses of the scattering cross-sections. One can verify the validity of the WKB approximation in both cases by verifying the conditions of validity of the WKB approximation (Merzbacher 1970) namely

$$\lambda(r)|(dp/dr)| \ll |p(r)|,$$

where $\lambda(r)$ and $p(r)$ are the wavelength and momentum at position r. Table 2 illustrates this for r in the surface region for the two cases referred above. It is clear that the ratio $\lambda(r)|(dp/dr)|/|p(r)| \approx 10^{-2}$ is quite satisfactory for the validity of the WKB approximation. This indicates that it is quite appropriate to use the WKB approximation. The condition for the validity of the WKB approximation (Merzbacher 1970) is obtained by neglecting $k'(r)$ (i.e. $(d/dr)k(r)$) when compared to $k^2(r)$ in the leading order ($n = 0$) WKB approximation which results in the standard formula for phase shift that is generally used. In the antiproton-nucleus and nucleus-nucleus scattering that we consider, the condition $k^2(r) \gg k'(r)$ is valid in the region of interest. The effect of incorporating higher order WKB approximation has been studied by Chan *et al* (1981) which shows that the

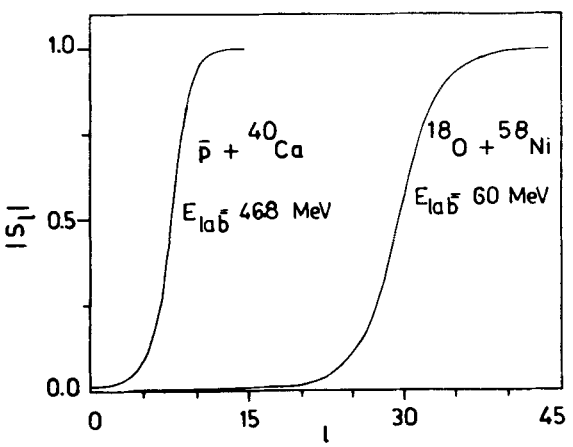

Figure 2. Comparison of reflection functions as a function of angular momentum for $^{18}O + {}^{58}Ni$ at $E_{lab} = 60$ MeV and $\bar{p} + {}^{40}Ca$ at $E_{lab} = 46{\cdot}8$ MeV. Potential parameters are given in table 1.

leading order WKB approximation is adequate for the simple parametric description of the scattering data. Another remarkable similarity between the heavy-ion scattering and $\bar{p}$-nucleus scattering is illustrated in figure 2 where we compare the reflection functions corresponding to the two cases namely $^{18}O + {}^{58}Ni$ and $\bar{p} + {}^{40}Ca$. Both processes being surface-dominated phenomena, the reflection function rises quite rapidly near the grazing angular momentum. Based on these observations, we formulate in the next section analytical expressions of the nuclear phase-shift using the one-turning point WKB approximation and the mathematical techniques given by Shastry (1982).

3. Approximate closed-form expression for phase-shift

We now consider antiproton-nucleus potential. The effective real potential for the lth partial wave has, in general, only one turning point. This turning point becomes complex when the complex effective potential (including imaginary part) is used. The one-turning point WKB formula for nuclear phase-shift is given by

$$\delta_N(\lambda) = \lim_{R\to\infty}\left(\int_{r_1}^{R}(k^2 - V_n(r) - V_c(r) - V_\lambda(r))^{1/2}\,dr - \int_{r_c}^{R}(k^2 - V_c(r) - V_\lambda(r))^{1/2}\,dr\right), \tag{4}$$

where

$$k^2 = (2\mu E/\hbar^2), \quad V_n(r) = (2\mu/\hbar^2)U_n(r), \quad V_c(r) = (2\mu/\hbar^2)U_c(r),$$
$$V_\lambda(r) = \lambda^2/r^2 \quad \text{and} \quad \lambda = l + \tfrac{1}{2}.$$

Here E is the centre of mass energy. Here r_1 is the complex turning point and r_c is the turning point when the nuclear potential is switched off. The expression for r_c is given by

$$\begin{aligned} r_c &= (\eta + (\lambda^2 + \eta^2)^{1/2})/k && r_c \geqslant R_c \\ &= ((-x + y)/(2\eta k/R_c^3))^{1/2} && r_c \leqslant R_c, \end{aligned} \tag{5}$$

where

$$\eta = -Z_T e^2 \mu/\hbar^2 k$$
$$x = (k^2 R_c - 3k\eta)/R_c$$

and

$$y = (x^2 + 4\lambda^2 \eta k/R_c^3)^{1/2}.$$

For all the partial waves for which $r_c > R_r$, R_i we can use the method developed by Shastry (1982). We write

$$\delta_N(\lambda) = \delta_N^{(1)}(\lambda) + \delta_N^{(2)}(\lambda), \tag{6}$$

where $\delta_N^{(1)}(\lambda)$ gives the contribution to $\delta_N(\lambda)$ in the range r_c to ∞ and $\delta_N^{(2)}(\lambda)$ gives the

contribution in the range r_1 to r_c. The expression for $\delta_N^{(1)}(\lambda)$ becomes

$$\operatorname{Re}\delta_N^{(1)}(\lambda) = -\left(\frac{2\mu V_0}{\hbar^2}\right)\frac{1}{2k^2}\left\{\sum_{n=0}^{\infty}\left[-\exp\left(\frac{-\eta + kR_r}{ka_r}\right)\right]^{n+1}\right.$$
$$\times\left[\eta K_0\left(\frac{n+1}{ka_r}(\lambda^2+\eta^2)^{1/2}\right) + (\lambda^2+\eta^2)^{1/2}\right.$$
$$\left.\left.\times K_1\left(\frac{n+1}{ka_r}(\lambda^2+\eta^2)^{1/2}\right)\right]\right\}, \tag{7}$$

where K_i is the K-type modified Bessel function (Abramowitz and Stegun 1964).

We can write a similar expression for Im $\delta_N^{(1)}(\lambda)$ by simply replacing the parameters of the real potential with the corresponding parameters of the imaginary potential. If one approximates the complex turning point r_1 by $r_1^{(1)}$ given by

$$r_1^{(1)} = r_c - f(r_c)/f'(r_c), \tag{8}$$

where

$$f(r) = r^2 - \frac{2\eta}{k}\cdot r - \frac{\lambda^2}{k^2} - \frac{r^2}{k^2}V_n(r) \tag{9}$$

one can get a reasonable approximation to $\delta_N^{(2)}(\lambda)$ given by

$$\delta_N^{(2)}(\lambda) = \tfrac{1}{2}r_c^3\frac{(-V_n(r_c))^{3/2}}{(k^2r_c^2 + \lambda^2 - \varepsilon)}, \tag{10}$$

where

$$\varepsilon = r_c\frac{\mathrm{d}}{\mathrm{d}r}(r^2V_n(r))|_{r=r_c}.$$

Hence, in this approach it is not essential to calculate the exact turning point. However, if one computes the exact turning point, the expression for $\delta_N^{(2)}(\lambda)$ in the linear approximation becomes

$$\delta_N^{(2)}(\lambda) = \tfrac{1}{2}(r_c - r_1)(-V_n(r_c))^{1/2}. \tag{11}$$

The exact turning point is calculated by carrying out the Newton-Raphson method of iteration till the saturation is reached. We have found that 4 to 5 iterations are adequate to get the exact turning point. For real potential, the turning point separates the classically allowed region from the forbidden region. The generalization of this to complex potentials has been used in the study of heavy-ion scattering (see for example, Brink 1985). In figures 3a and 3b, we have plotted the Coulomb turning point r_c, the exact complex turning point r_1 and $r_1^{(1)}$, the first iteration value of r_1 for $\bar{p} + {}^{40}\mathrm{Ca}$ at $E_{\mathrm{lab}} = 46{\cdot}8$ MeV. The figure indicates that for most of the partial waves except for a few, $r_1^{(1)}$ is quite a good approximation to r_1. The turning points obtained in the interior region for $l < 7$ by first iteration are not close to the exact turning points. But the smaller partial waves are highly absorptive ($|S_l| \simeq 0$) and the scattering data are not very sensitive to the potential in the interior region. Hence, some error in the calculation of the turning point does not significantly affect the cross-sections as far as the partial waves which are more or less fully absorbed are concerned. We use the expressions given above for $\delta_N^{(1)}(\lambda)$ and $\delta_N^{(2)}(\lambda)$ to compute the nuclear phase-shift.

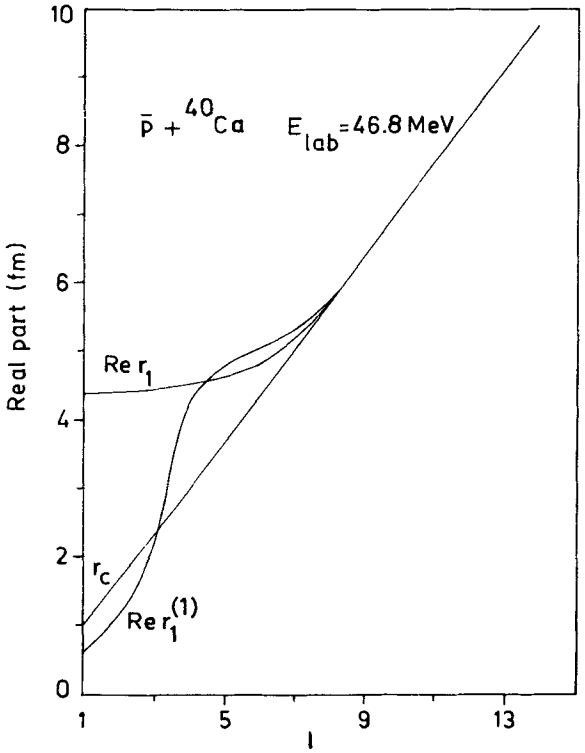

Figure 3a. Variation of the real part of complex turning point as a function of l along with r_c and the result of first iteration for real r_1 denoted by $r_1^{(1)}$. The potential parameters are given in table 1.

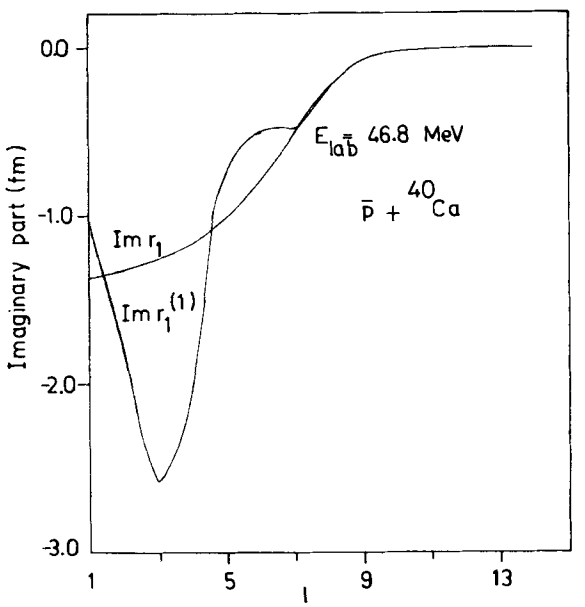

Figure 3b. Variation of the imaginary part of the turning point as a function of l. Potential parameters are given in table 1.

Since the arguments of the functions K_0 and K_1 appearing in (7) are generally large we can approximate K_0 and K_1 by their asymptotic expansions which are given by Abramowitz and Stegun (1964):

$$K_0(x) = x^{-1/2}\exp(-x)\sum_{n=0}^{6} a_n(2/x)^n + \varepsilon_1, |\varepsilon_1| < 1{\cdot}9 \times 10^{-7},$$

$$K_1(x) = x^{-1/2}\exp(-x)\sum_{n=0}^{6} b_n(2/x)^n + \varepsilon_2, |\varepsilon_2| < 2{\cdot}2 \times 10^{-7}.$$

One may note that the formula developed can be readily used to compute the antiproton-nucleus scattering to fit the cross-section data by suitably varying the parameters. This approach is similar to the closed-formalism developed by Frahn and Rehm (1978). In the next section we give typical values of the data used in our calculation.

4. Calculations and discussion

In order to demonstrate the usefulness of the WKB technique in analysing the $\bar{p}$-nucleus scattering, we have studied two typical cases: $\bar{p} + {}^{12}C$ at $E_{lab} = 46{\cdot}8$ MeV and $\bar{p} + {}^{40}Ca$ at $E_{lab} = 46{\cdot}8$ MeV for which cross-sections have been measured and optical model fits have been obtained. In figure 4, we show the reflection functions obtained by optical model fits and compare them with those obtained by the WKB approximation using both the approximate expression for the WKB turning point and the numerically evaluated turning point. This indicates fairly good agreement with the reflection functions obtained using the optical model calculations for both $\bar{p} + {}^{12}C$ and $\bar{p} + {}^{40}Ca$. The differential cross-sections for $\bar{p} + {}^{12}C$ scattering and $\bar{p} + {}^{40}Ca$ are shown in

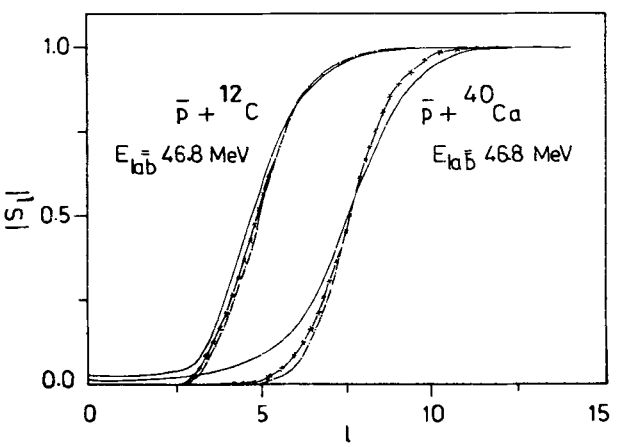

Figure 4. Reflection functions for $\bar{p} + {}^{12}C$ and $\bar{p} + {}^{40}Ca$ obtained by using the exact optical model calculation (—) and those obtained by using $\delta_N(\lambda) = \delta_N{}^{(1)}(\lambda) + \delta_N{}^{(2)}(\lambda)$ with $\delta_N{}^{(2)}(\lambda) = \frac{1}{2}(r_c - r_1{}^{(1)})(-V_n(r_c))^{1/2}$ (— × — × —), and using $\delta_N(\lambda) = \delta_N{}^{(1)}(\lambda) + \delta_N{}^{(2)}(\lambda)$ where $\delta_N{}^{(2)}(\lambda)$ is given by equation (11) (—·—·—). Potential parameters are given in table 1.

figures 5 and 6 where we have plotted the cross-sections obtained by using optical model calculations and the cross-sections generated by the one-turning point WKB approximation. As the cross-sections based on optical model give fairly good fit to the experimental data the optical model prediction can be taken to represent the experimental data. Hence, in figures (5) and (6) the cross-sections generated by the one-turning point WKB approximation have been compared with the optical model predictions. Our result shows that the WKB approach is adequate to describe the essential features of the cross-sections. This shows that the semi-classical WKB approach is fairly suitable for $\bar{p}$-nucleus scattering and hence can be adopted to analyse the $\bar{p}$-nucleus scattering amplitude and scattering cross-sections in the same way as one does in the heavy-ion scattering. The primary difference, however, is that in $\bar{p}$-nucleus scattering the one-turning point WKB formula is quite adequate and the number of partial waves involved is smaller as compared to that in the heavy-ion scattering. Further, the similarity in the reflection functions and closed-form expression for WKB integrals indicates that closed-formalism approach of Frahn can also be successfully

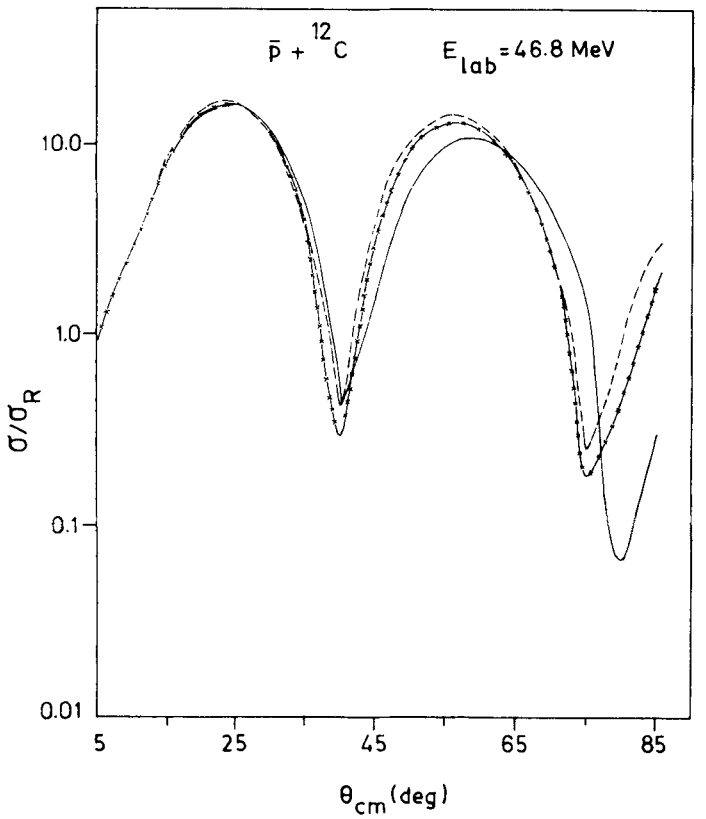

Figure 5. The ratio of differential cross-section to the Rutherford cross-section as a function of angle (in the centre of mass system) for $\bar{p} + {}^{12}C$ at $E_{lab} = 46{\cdot}8$ MeV obtained by using optical model calculation (—) and those obtained by using $\delta_N(\lambda) = \delta_N{}^{(1)}(\lambda) + \delta_N{}^{(2)}(\lambda)$ with $\delta_N{}^{(2)}(\lambda) = \frac{1}{2}(r_c - r_1{}^{(1)})(-V_n(r_c))^{1/2}$ (— × — × —) and using $\delta_N(\lambda) = \delta_N{}^{(1)}(\lambda) + \delta_N{}^{(2)}(\lambda)$ where $\delta_N{}^{(2)}(\lambda)$ is given by equation (11) (—·—·—).

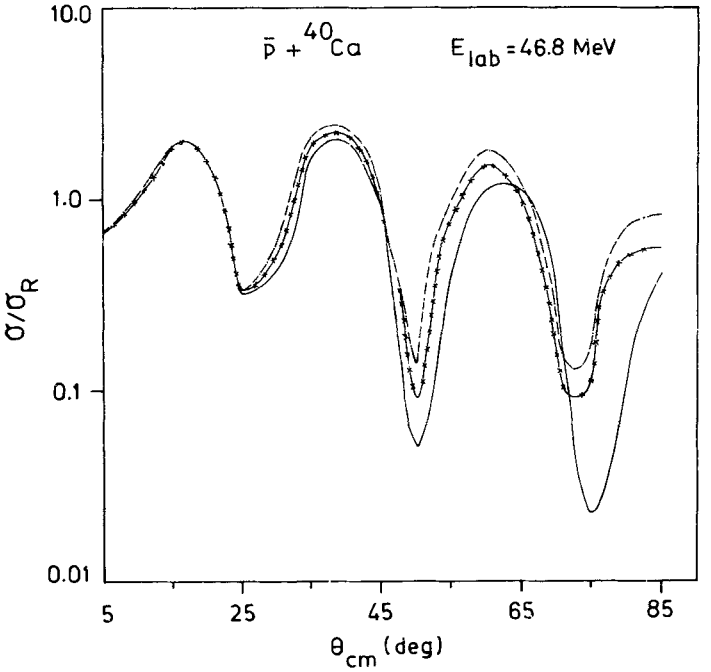

Figure 6. Same as figure 5 for $\bar{p} + {}^{40}Ca$ at $E_{lab} = 46{\cdot}8$ MeV.

employed for the analysis of $\bar{p}$-nucleus scattering. At present the $\bar{p}$-nucleus scattering data are confined to the centre of mass angle $\theta \leqslant 65°$. When extended data for higher angles are available new features may come up which will necessitate more elaborate analysis of the scattering data using quantum-mechanical and semiclassical methods.

Acknowledgements

One of the authors (CSS) is grateful to Professors M K Pal and S Mukherjee for providing useful facilities to him during January and February 1987 at the Saha Institute of Nuclear Physics, Calcutta where part of this work was completed.

References

Abramowitz M and Stegun I A 1964 *Handbook of mathematical functions* (New York: Dover) p. 374
Brink D M 1985 *Semi-classical methods in nucleus-nucleus scattering* (Cambridge, London, New York, New Rochelle, Melbourne, Sydney: Cambridge University Press) p. 31
Chan C K, Subeka P and Lu P 1981 *Phys. Rev.* **C24** 2035
Frahn W E and Rehm K E 1978 *Phys. Rep.* **37** 1
Garreta D, Birien P, Bruge G *et al* 1984 *Phys. Lett.* **B135** 266
Heiselberg A, Jensen A S, Miranda A, Oades G C and Dumbrajs O 1985 *Nucl. Phys.* **A446** 637
Ingemarsson A 1986 *Nucl. Phys.* **A454** 475
Janouin S *et al* 1986 *Nucl. Phys.* **A451** 541

Kronenfeld J, Gal A and Eisenberg J M 1984 *Nucl Phys.* **A430** 525
Kubo K I, Toki H and Igarashi M 1985 *Nucl. Phys.* **A435** 708
Mackellar A D, Satchler G R and Yong C Y 1984 *Z. Phys.* **A316** 35
Merzbacher E 1970 *Quantum mechanics* (New York, Chichester, Brisbane, Toronto: John Wiley) Chap. 7
Shastry C S 1982 *J. Phys.* **G8** 1431
Videbaek F, Christensen P R, Hansen O and Ulbak K 1976 *Nucl. Phys.* **A256** 30